Gapwaveguide Automotive Imaging Radar Antenna with Launcher in Package Technology

(article starts on next page)

Gapwaveguide Automotive Imaging Radar Antenna with Launcher in Package Technology

QIANNAN REN[1], (Graduate Student Member, IEEE), CARLO BENCIVENNI[2], GIORGIO CARLUCCIO[3], (Member, IEEE), HARSHITHA THIPPUR SHIVAMURTHY[3], ANTON DE GRAAUW[3], FEIKE JANSEN[3], JIAN YANG[1], (Senior Member, IEEE), ASHRAF UZ ZAMAN[1], (Senior Member, IEEE)

[1]Department of Electrical Engineering, Chalmers University of Technology, Gothenburg, 412 96 Sweden
[2]Gapwaves AB, Gothenburg, 412 63 Sweden
[3]NXP Semiconductors, Eindhoven, 5656 AG The Netherlands

Corresponding author: Qiannan Ren (e-mail: qiannan@ chalmers.se).

ABSTRACT A 77 GHz gapwaveguide radar antenna system with launcher-in-package (LiP) technology is presented in this paper for automotive imaging applications. Firstly, state-of-the-art LiP technology integrated with radar transceivers is proposed. The transceivers are equipped with waveguide interfaces for RF connection, enabling direct integration with waveguide antennas. Robust interconnects for coupling transceivers to waveguide antennas with non-galvanic contacts are proposed using gapwaveguide packaging technology. A simultaneous multi-mode imaging radar system using 4 cascaded aforementioned transceivers is introduced. Designated antenna elements of the system are realized by slot arrays with center-fed ridge gapwaveguides. Ultimately, the imaging radar antenna has a top radiating slot layer, a middle distribution layer and a bottom interconnect layer capable of accommodating 4 LiP radar transceivers with considerable assembly tolerance which is really one of the key aspects for commercial automotive radar applications. Input matching and radiation patterns of the antenna are verified by measurement. The results indicate that the proposed gapwaveguide imaging radar antenna in conjunction with the novel LiP packaging is able to serve the radar system properly. To the best of the authors' knowledge, the proposed gapwaveguide antenna system is the first imaging radar antenna system ever developed for LiP components. This work provides a compact, high-efficiency and cost-effective solution for the integration of complex radar systems with waveguide antennas.

INDEX TERMS imaging radar, automotive, launcher-in-package, transceiver, gapwaveguide, slot array.

I. INTRODUCTION

FULLY autonomous vehicles are able to drive independently by heavily relying on sensor data. This poses tremendous challenges on the perception sensors in terms of target classification, environmental adaptability, etc. Widely used sensors, such as radar, light detection and ranging (LIDAR), ultrasonic, have their strengths and weaknesses under different scenarios [1], [2]. Radar sensors are able to measure the instantaneous velocity and handle poorly lighted environments, but constrained by limited resolution in direction of arrival (DoA) estimation. The latest radar sensing systems, commonly referred to as imaging radars (IMRs), are

capable of achieving high angular resolution in both azimuth and elevation direction [3], [4]. IMRs typically utilize multi-input and multi-output (MIMO) antenna systems which can provide a cost-effective approach to improve angular resolution of the radar by multiplexing transmissions across a number of antennas [5].

Previously, automotive radars operating at 77 GHz band (76-77 GHz) were mainly for long-range radar (LRR) applications such as adaptive cruise control (ACC). However, medium-range radar (MRR) and short-range radar (SRR) applications are compatible with 77 GHz band as well [6]–[8]. Thus, it is of high interest to develop multi-mode IMR systems at 77 GHz
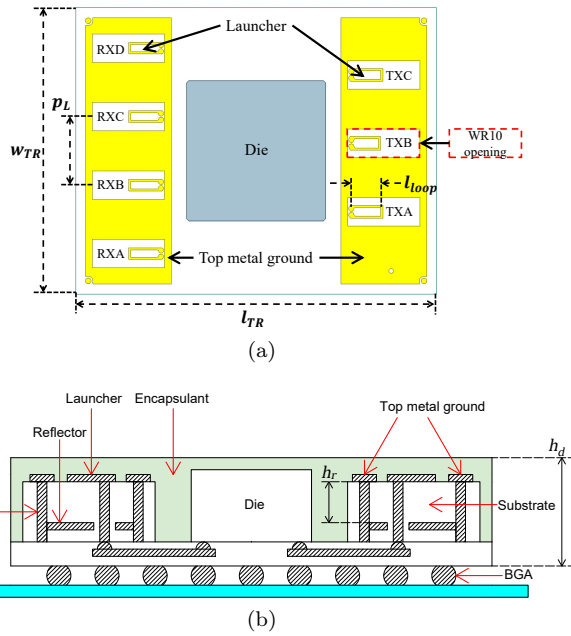
FIGURE 1. LiP transceiver equipped with 4 RXs and 3 TXs: (a) layout of the top metal layer; (b) sectional view of the transceiver [17].

band. Previous work [9] presents an imaging radar capable of operating in triple modes simultaneously. In this work, advanced design of the antenna system using gapwaveguide technology is proposed. Gapwaveguide technology is widely used for multi-layer antenna designs [10]–[12]. It features non-galvanic contact between the layers, thereby ensuring higher reliability of assembly and robustness of the design at millimeter wave frequency band.

Nowadays, almost all radar sensing systems are based on highly integrated system-in-package (SiP) components featuring multiple transmitters (TX) and receivers (RX) with functionalities from radio frequency (RF) front-end to intermediate frequency (IF) signal processing. Embedded wafer level ball grid array (eWLB) is one of the advanced packaging technologies for such radar transceivers [13]. It can provide components with flip-chip assembly which is favorable for applications based on print circuit board (PCB). This leads logically to PCB antenna being the most widely used antenna connected to the transceiver. However, dielectric loss will deteriorate the RF performance especially when complex antenna systems are used [14], [15]. PCB antennas also lack flexibility for routing of the feeding lines and placement of the antenna elements. Therefore, waveguide antenna placed on top of the transceivers becomes a better candidate to implement a complex antenna system operating at high frequency for next generation automotive radar and sensing applications [12], [16].

In general, to connect the transceivers to waveguide antennas, intermediate transitions on PCB are used

[18]–[20]. Additional insertion loss and PCB board space consumption of the transition result in a cumbersome design that wears down the potentials of waveguide antennas. Hence, SiP components with waveguide interfaces that are able to connect waveguide antennas directly have been investigated lately [21]. As depicted in Fig. 1, such packaging technologies are referred to as launcher in package (LiP) [17]. The waveguide transitions, here named as waveguide launchers, are realized inside the SiP component by means of eWLB process.

Certainly, LiP components demand compact and robust interconnections to the waveguide antennas. In addition, the interconnection should be friendly for assembly considering the fragile LiP components. Gapwaveguide packaging technology utilizes periodic pins to realize a band gap covering the frequency band of interest, ensuring high isolation along with non-galvanic connections which is advantageous for flexible mechanical assembly [22].

This paper presents a cutting-edge design of automotive imaging radar system based on high-efficiency fully metallic waveguide antennas. The main novelties of the presented work are listed below:

1) A fully functional automotive imaging radar antenna system based on gapwaveguide technology is developed in conjunction with the LiP based automotive radar transceivers at 77 GHz. For the first time, the LiP technology is proposed on system level by providing a feasible solution for the integration of waveguide antenna with active circuits. In addition, advantages of LiP technology, in terms of performance (energy-efficient due to the elimination of external waveguide transitions) and cost (able to avoid using costly RF substrate) are validated.

2) Highly integrated automotive radar transceiver equipped with 4 RXs and 3 TXs is firstly presented providing compact waveguide interfaces via the proposed LiP technology, in contrast to previous publications only presenting passive validations on a solitary transition [21], [23]–[25].

3) Gapwaveguide based contact-less waveguide interconnect is firstly employed for the connection to LiP components.

4) Novel rectangular waveguide (RW) to ridge gapwaveguide (RGW) transition is proposed with compact periodicity, able to address the challenges of fan-out of the LiP component.

5) Despite the fact that waveguide antennas are of high interest for industrial automotive radar applications recently, there are limited examples or research publications on integrated waveguide-based antenna system with elements at highly sparse locations over a large aperture [26]. It is quite challenging for the assembly of conventional waveguides which are normally fabricated by E- or

H-plane split blocks, considering certain feeding lines of the proposed antenna elements are with lengths up to 120 mm (approximately 30 wavelengths at 77 GHz) [27]. The proposed gapwaveguide antenna system is proved to be a better low-cost candidate for implementation of such large-aperture antenna systems integrated with numbers of cascaded transceivers.

This paper is organized as follows. LiP components and gapwaveguide interconnects are introduced in Section II. Compact transitions to the antenna distribution layer are described in Section III. Design of gapwaveguide antennas is given in Section IV. Measurements of the interconnects and the imaging radar antenna are presented in Section V and Section VI, respectively. Finally, conclusions are given in Section VII.

II. DESIGN OF GAPWAVEGUIDE INTERCONNECT FOR LIP

The LiP integrated circuit preceding the antenna design in this work is a transceiver with 3 TXs and 4 RXs, covering 76 to 81 GHz band and supporting SRR, MRR, LRR applications including high resolution IMRs [17], [28]. Layout of the waveguide launchers is shown in Fig. 1. Compact neighboring transitions based on loops that are fed by differential lines are proposed [17], in contrast to the designs in [21], [23]–[25] that only present solitary transitions based on vias, tapered lines or ring slots. Thanks to the multi-layer features of eWLB packaging with embedded substrates, the waveguide launchers can present RF ports at the top while the ball grid array at the bottom provides other connections to the transceiver. The LiP component can realize high-efficiency integration with waveguide antennas by eliminating the external waveguide transitions. Moreover, the LiP component is able to avoid using high performance RF substrates. This gives significant cost benefits in designing the complex imaging radar modules with multiple transceivers operating at 77 GHz.

Compact, robust and assembly-friendly waveguide interconnects between LiP components and antennas with RW interfaces are proposed based on gapwaveguide packaging, as shown in Fig. 2. The staggered pins above the top metal ground with dielectric encapsulant ($\epsilon_r = 3.65$, [29]) will create a stop band preventing the field from leaking through the air gap. The stop band is determined by plotting the dispersion diagram over the irreducible Brillouin zone (Γ-X-M-Γ) with periodic boundary conditions in x and y directions, as shown in Fig. 3. The dispersion diagram of the unit cell is shown in Fig. 4. The stop band is from 65 to 130 GHz with an air gap of 100 μm. As a result, the large stop band is able to guarantee robustness of the interconnect.

The launcher is optimized together with the interconnect for a better performance. By replacing the die with matched loads, reflection coefficients and isolation of the RW ports are simulated. Manufacturing tolerances of the
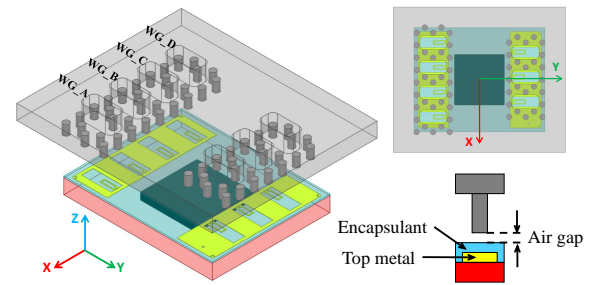

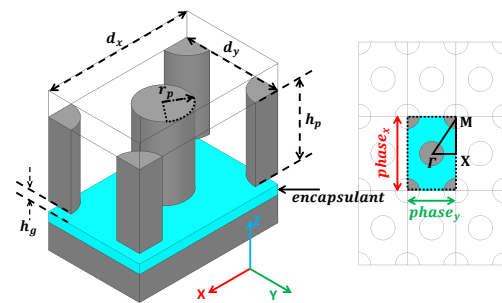**FIGURE 2. Compact gapwaveguide interconnects for the LiP transceivers.**

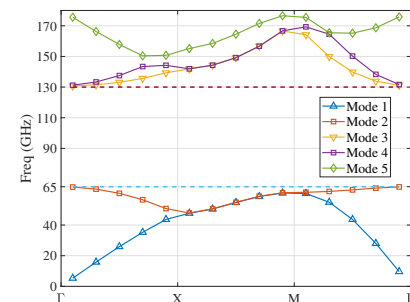**FIGURE 3. Gapwaveguide pin texture adopted by the interconnect.**

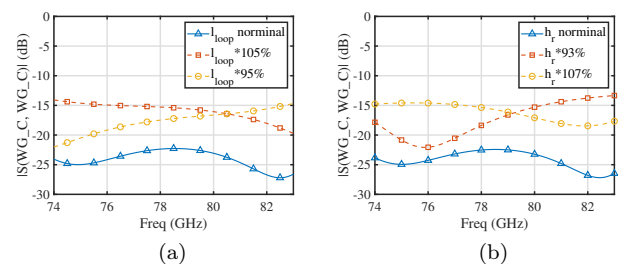**FIGURE 4. Dispersion diagram of the gapwaveguide pin texture.**

FIGURE 5. Manufacturing tolerances of the launcher regarding (a) the loop length (l_{loop}) and (b) substrate thickness (h_r).

launcher regarding the loop length (l_{loop}) and substrate thickness (h_r), which are considered as the most critical parameters, are investigated by examining the variation of matching, as shown in Fig 5. Assembly tolerance in terms of air gap variation and misalignment in x and
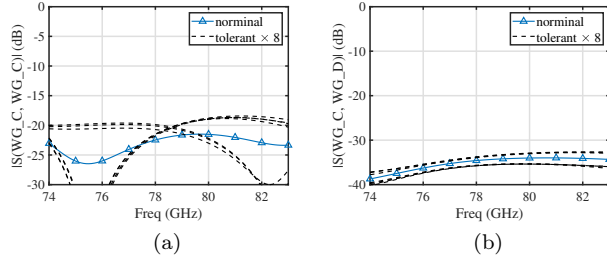
FIGURE 6. Simulated results of the interconnects considering ±50 μm misalignment in both *x* and *y* direction, plus ±50 μm air gap variation, in total of 8 scenarios besides the nominal.
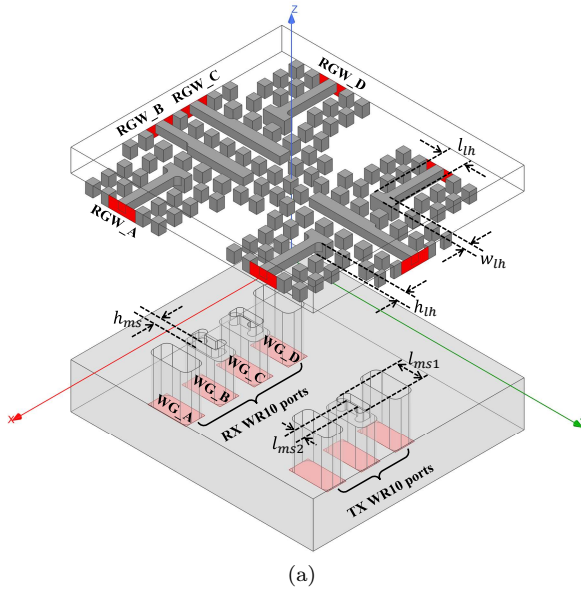

FIGURE 7. Compact transitions from the interconnects to the distribution layer: (a) 3D view, (b) top view.

y directions are tested as well. As shown in Fig. 6, the interconnects have reflection coefficients better than -20 dB and isolation larger than 30 dB between the adjacent RW ports, while featuring robust performance over 74 to 83 GHz. The proposed gapwaveguide interconnect features non-galvanic contact, as well as high isolation when the transitions are placed in close proximity.
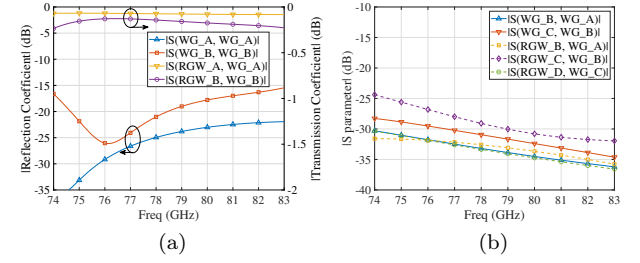

FIGURE 8. Input matching (a) and port isolation (b) of the compact transitions for RXs.
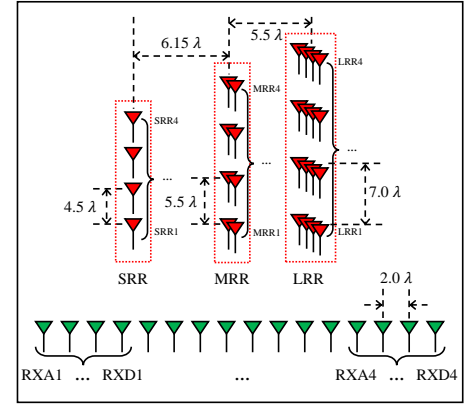

FIGURE 9. Antenna system of the simultaneous multi-mode automotive IMR with 12 TXs and 16 RXs [9].

III. DESIGN OF COMPACT TRANSITIONS FOR ANTENNA FEEDING NETWORKS

RGW is employed for the feeding networks of the antenna, due to its compact and broadband properties. Thus, the challenge becomes implementing compact transitions from RW to RGW after the interconnect. Considering the placement of RW ports, transitions from the broadside of RW have been utilized for the lateral ports, as depicted in Fig. 7. For the ports in the middle, more compact longitudinal slots based transitions have been used. The longitudinal slots are placed approximately quarter guided wavelength away from the short end of RGW, and shaped like a conventional ridge waveguide which helps to achieve good impedance matching and wide bandwidth. Considering the resemblance between RX and TX transitions, simulated results of the RX transitions are discussed here exclusively. The reflection coefficients are better than -25 dB for the lateral transitions and less than -20 dB for the middle transitions from 75 to 78 GHz, as shown in Fig. 8a. Side-by-side isolation between the neighboring RW ports and forward isolation between the adjacent RW and RGW are larger than 25 dB as shown in Fig. 8b.

IV. SYSTEM SPECIFICATION AND ANTENNA IMPLEMENTATION

TABLE 1. Dimensions of the design

Parameters	Dimension (mm)	Parameter	Dimension (mm)
Launcher Design [17]			
w_{TR}	9.5	l_{TR}	12
p_L	2.27		
Interconnect Design			
d_x	1.52	d_y	1
h_p	0.8	r_p	0.25
h_g	0.1		
Transition Design			
h_{lh}	0.82	l_{lh}	1.42
w_{lh}	0.50	h_{ms}	0.51
w_{ms1}	0.89	l_{ms1}	1.72
w_{ms2}	0.54	l_{ms2}	0.75
Antenna Design			
L_{st}	2.25	D_{st}	2.63
H_{dr}	0.93	L_{dr}	2
W_{dr1}	0.47	W_{dr2}	0.86
W_{dr3}	1.76	l_{ST}	2.29
d_{ST}	2.99	h_{DR}	0.72
l_{DR}	1.78	w_{DR1}	0.54
w_{DR2}	0.83	w_{DR3}	1.67
w_1	0.83	w_2	0.5
w_3	0.81	w_4	0.5
w_5	0.5	d_1	2.5

TABLE 2. Specifications of the IMR

Parameters		SRR	MRR	LRR
Distance	Maximum	75 m	150 m	250 m
	Resolution	0.3 m	0.6 m	1.2 m
Velocity	Min/Max	-280 / 280 km/h		
	Resolution	0.16 m/s	0.08 m/s	0.08 m/s
DoA	AZ HPBW	1.6°		
	AZ FoV	±60°	±30°	±15°
	EL HPBW	±2.8°	±2.25°	±1.8°
	EL FoV	6°		

Note: Azimuth (AZ), Elevation (EL), Half Power Beam Width (HPBW), Field of View (FoV).

TABLE 3. Specifications of the IMR Antenna

Antenna	Freq. (GHz)	BW (GHz)	Gain (dBi)	HPBW AZ (deg)	HPBW EL (deg)
RX	76.5	> 1	15	60	10
TX SRR	76.5	> 1	10	60	16
TX MRR	76.5	> 1	16	36	16
TX LRR	76.5	> 1	19	18	16

A. SYSTEM TARGET SPECIFICATIONS

A simultaneous multi-mode automotive IMR with 12 TXs and 16 RXs has been proposed in the previous work [9]. The specifications of the IMR are shown in Table. 2. Most commonly used multiplexing technique in automotive radar applications is time division multiplexing (TDM) as a result of its simple and cost-effective implementation [30]. However, as the pulse repetition interval (PRI) of the same transmitter increases with TDM, the maximum unambiguous velocity is decreased by a factor of number of transmitting antennas. This is particularly challenging for IMRs with tens of transmitters. Compared with TDM, doppler division multiplexing (DDM) where transmitted signals are orthogonally separated with frequency offsets in the Doppler dimension, are able to maintain the maximum unambiguous velocity with increasing transmitters [31], [32]. However, the simultaneous transmission of DDM will consume more power, thus pose challenges on the heat dissipation and reliability of the system. Previous work [9] based on a combination of TDM MIMO and DDM MIMO has shown a trade-off between maximum unambiguous velocity and power consumption. The layout of the antenna system is shown in Fig. 9. It consists of 16 identical RX antennas separated by 2 free space
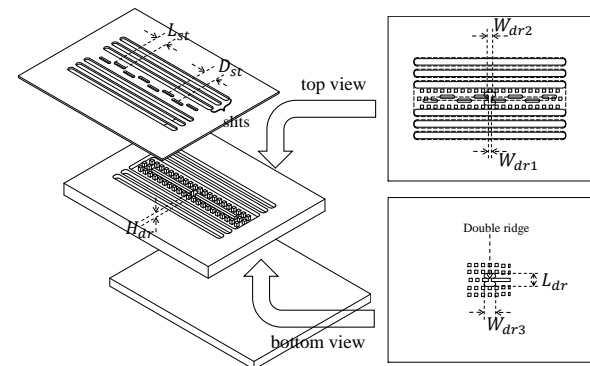

FIGURE 10. RX slot array using gapwaveguide with top view and bottom view.

wavelength (λ) at center frequency. The TX arrays assign 4 elements to each mode with unique FoV in azimuth direction. Utilizing 4 radar transceivers, each equipped with 3 TXs and 4 RXs, the IMR can implement high angular resolution in both AZ and EL directions.

B. DESIGN OF GAPWAVEGUIDE SLOT ARRAYS

Based on the system target performances, specifications of the antenna elements are determined, as listed in Table. 3. Gapwaveguide slot arrays are utilized for the antenna implementation. Antenna element of the RXs is realized by a linear array with 8 equally displaced longitudinal slots as shown in Fig. 10. Center-fed RGW line with a double-ridge section brings about a com-
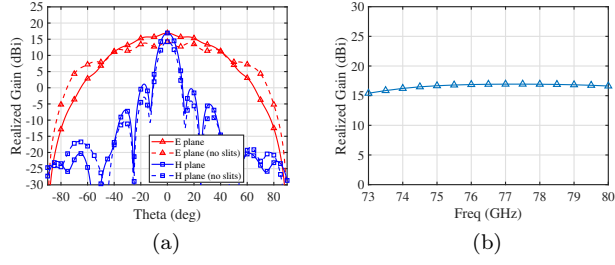
FIGURE 11. Simulated results of the RX antenna: (a) radiation pattern at 76.5 GHz, (b) realized gain at boresight direction over frequency.
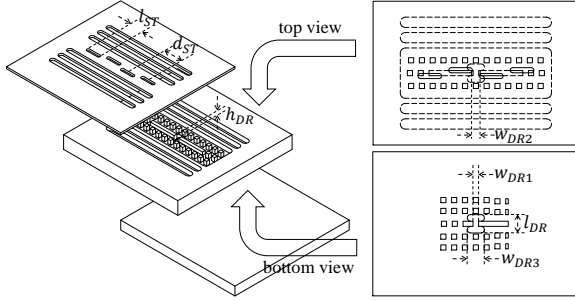

FIGURE 12. SRR slot array using gapwaveguide with top view and bottom view.

pact (capable of half-wavelength spacing placement) and broadband design. Considering the slot arrays will be implemented on a metal plate with numbers of neighboring elements, periodic slits are deployed on the lateral direction of the slots in order to reduce the finite ground plane edge diffraction, and also provide gain enhancement. Simulated E-plane (electric field polarization) and H-plane (magnetic field polarization) pattern of the RX antenna at 76.5 GHz are shown in Fig. 11a. Without the slits, the truncated ground plane will induce noticeable ripples in the E-plane pattern which would affect the consistency over RX elements. Realized gain of the RX element is larger than 16 dB at boresight direction, as shown in Fig. 11b.

TX antennas are realized by multiple columns of a linear array with 4 equally displaced longitudinal slots as depicted in Fig. 12. The SRR antenna has the simplest implementation, while the MRR antenna with two columns and LRR antenna with four columns demand feeding networks with equal power dividers, as shown in Fig. 13a and Fig. 13b. The imaging radar system demands specific crossing points among the E-plane patterns of SRR, MRR and LRR antennas, as shown in Fig. 14a [9]. Simulated realized gains of the TX antennas at boresight direction are shown in Fig. 15.

The complete IMR antenna system with dimensions of 160 mm × 160 mm × 7 mm is shown in Fig. 16. The design consists of three layers: bottom interconnect layer, middle distribution layer and top radiating layer.
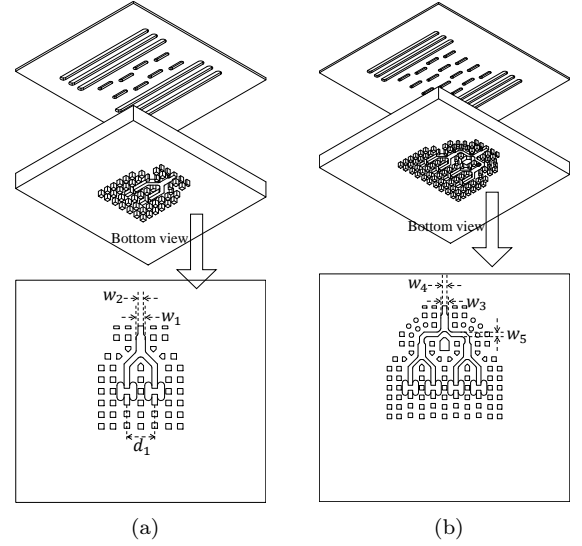

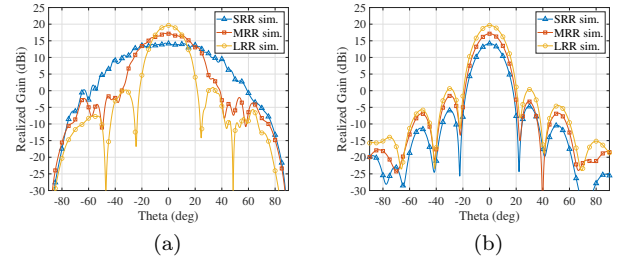**FIGURE 13.** MRR (a) and LRR (b) slot array using gapwaveguide with equal power dividers.

FIGURE 14. Simulated radiation pattern of the TX antennas at 76.5 GHz: (a) E-plane, (b) H-plane.
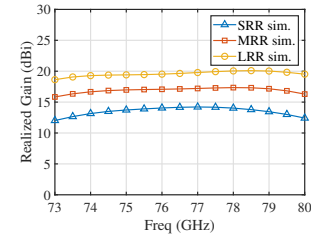

FIGURE 15. Simulated realized gains of the TX antennas at boresight direction over frequency.

Fig. 17 shows the detailed views of the IMR antenna. Two dummy elements are placed on the lateral sides of the RX array in order to mitigate the degradation of the edge elements performance. TX antennas are connected to particular transmitters with the shortest possible feeding lines. Due to the sparse locations of TX elements, lengths of the feeding lines are up to 30 wavelengths at 77 GHz. This demands gapwaveguide lines with low-loss characteristics. Simulated insertion loss of the RGW feeding line is approximately 0.186 dB/cm which agrees well with the measurement. Large aperture of
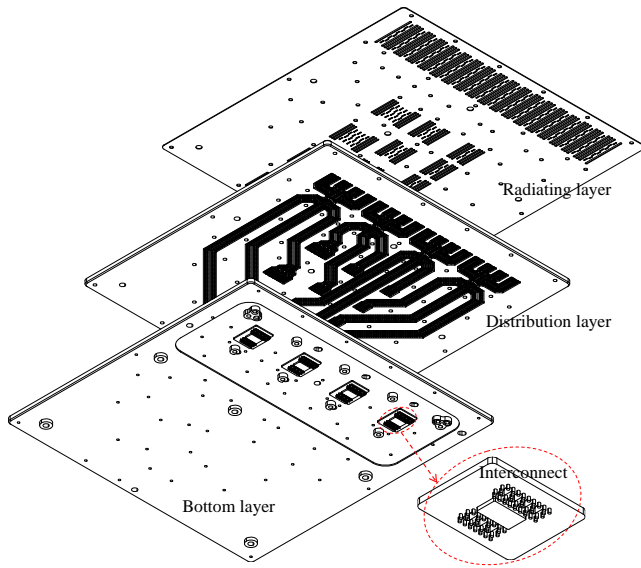
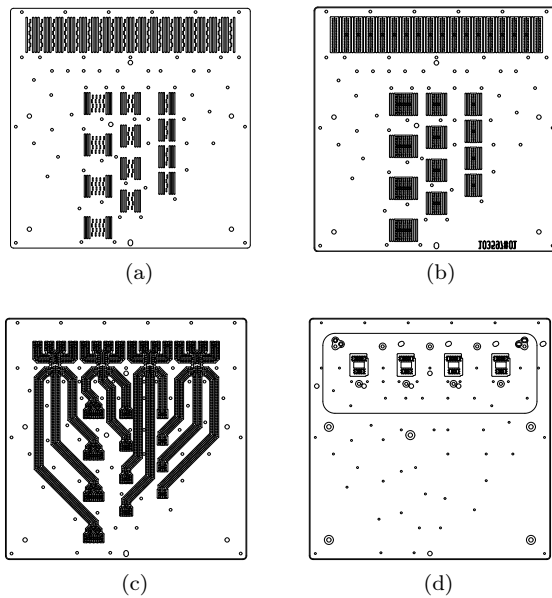**FIGURE 16.** Automotive imaging radar aiming for LiP technology.

FIGURE 17. Views of the imaging radar: (a) top view of the radiating layer; (b) top view of the distribution layer; (c) bottom view of the distribution layer; (d) bottom view of the bottom layer.

FIGURE 18. Testing structure for the interconnect and launcher: (a) configuration of RXs and TXs; (b) sectional view.
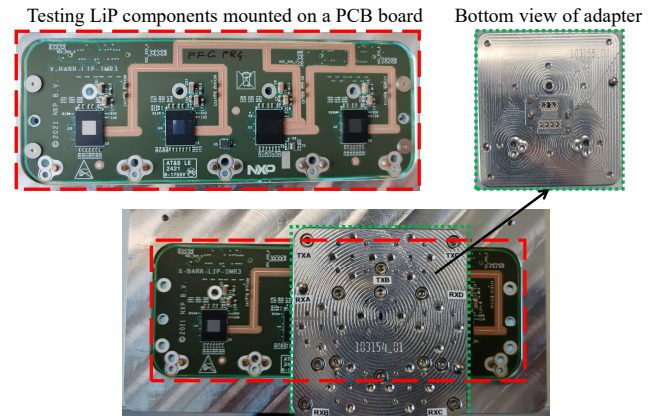
FIGURE 19. Testing LiP components with the adapter.

the antenna system is able to benefit advanced designs with better performance, however escalate the challenges on the assembly of multi-layer waveguide antennas. Gapwaveguide technology has been proved to be a better candidate for implementation of such antenna systems with large aperture. The antenna system has been validated by measurement and will be discussed in the next section.
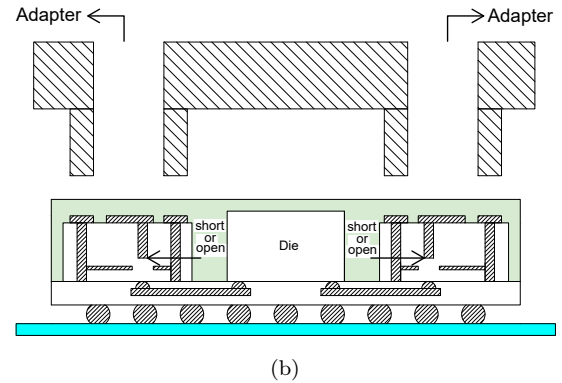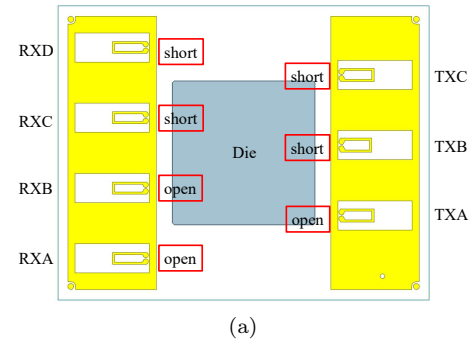
V. INTERCONNECT MEASUREMENT

To validate the launcher together with the interconnect, it has been chosen to tape-out the chips with launchers terminated by short or open loads, as shown in Fig. 18. Then, reflection coefficients are measured from the interconnect end. Such testing structures are capable of estimating the losses of the launcher together with interconnect, as well as the isolation under extreme scenarios of standing wave. A total of four transceiver units with the same configuration as indicated in Fig.

FIGURE 20. Measured reflection coefficients of the testing components with launchers terminated by short or open loads.

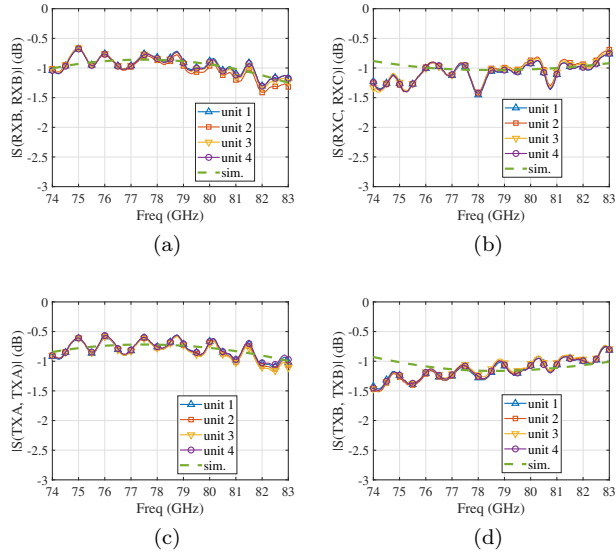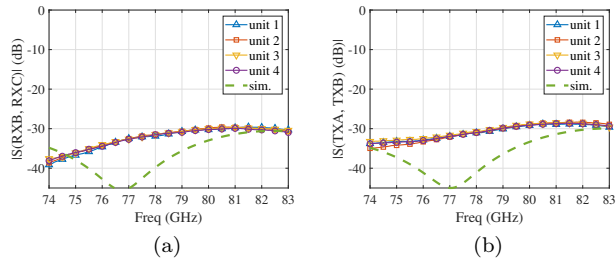**FIGURE 21.** Measured isolations of the testing components.

18a are measured. An adapter has been used during the measurement and eventually calibrated out from the results as shown in Fig. 19. Part of results are presented in Fig. 20 and Fig. 21. It has been shown that the dielectric and conductor loss of the testing structure is around 1 dB under standing wave operations. A similar insertion loss is obtained for the differential line to waveguide transition. According to the length of the differential line of each channel, additional dielectric losses need to be added, which lead to insertion loss performance comparable to the ones reported in [21]. The good agreement between the simulated and measured results is able to confirm the expected performance discussed in Section II, even though the measurement setup is for a strong reflection. The isolations between contiguous ports are larger than 30 dB even for a standing wave scenario.

VI. ANTENNA MEASUREMENT

The IMR antenna design discussed in Section IV has been fabricated by computer numerical control (CNC) milling in Aluminum as shown in Fig. 22. Layers of the
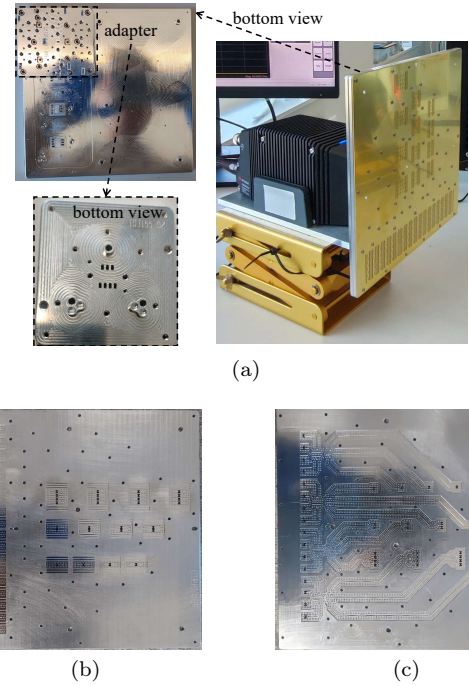
FIGURE 22. S-parameter measurement setup: (a) the IMR antenna prototype connected to a VNA, (b) distribution layer top view of the prototype, (c) distribution layer bottom view of the prototype.
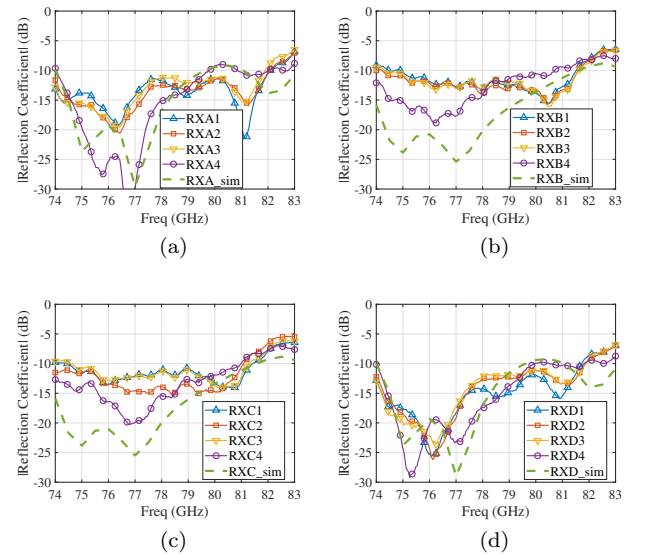
FIGURE 23. Reflection coefficients of RX slot arrays.

antenna are assembled by screws with the assistance of alignment pins. Due to the compact and irregular gapwaveguide interfaces, a similar waveguide adapter is utilized for the antenna measurement and eventually calibrated out as well. Fig. 23 shows that the reflection coefficients are better than -10 dB from 75 to 80 GHz for the RX antennas. Input impedance matching of the TX antennas are shown in Fig. 24. Under all the three operating modes, the measured reflection coefficients are

FIGURE 24. Reflection coefficients of TX slot arrays.

FIGURE 25. Measured radiation patterns of RX slot arrays at 76.5 GHz with all 16 elements plotted together: (a) E-plane, (b) H-plane.

FIGURE 26. Measured radiation patterns of TX slot arrays at 76.5 GHz: (a) SRR E-plane, (b) SRR H-plane, (c) MRR E-plane, (d) MRR H-plane, (e) LRR E-plane, (f) LRR H-plane.

better than -10 dB from 75 to 78 GHz.

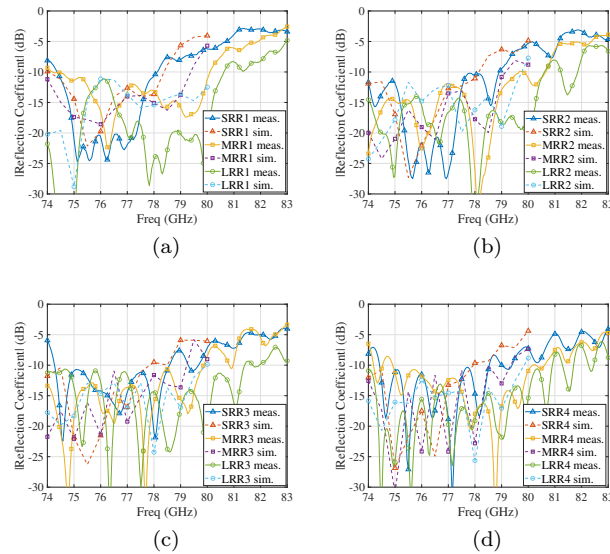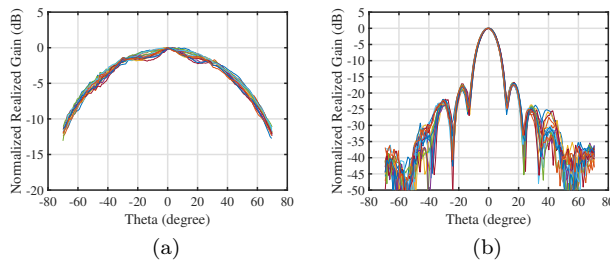Radiation patterns are measured in an anechoic chamber in far-field setup. E- and H-plane patterns of the 16 RXs at 76.5 GHz are plotted together, as shown in Fig. 25a and Fig. 25b. Realized gain of the RXs at boresight direction over frequencies are presented in Fig. 27a. It has been shown that the RX antennas have realized gain around 16 dBi with HPBW larger than 60° in AZ and 10° in EL. In addition, thanks to the slits on the sides of the slots, the patterns have shown excellent similarities among the 16 elements, which is one of the key aspect of such IMR application. Radiation patterns of the TX antennas are shown in Fig. 26. The patterns are able to fulfill the specifications of the IMR as listed in Table. 3. Realized gain of the TXs at boresight direction over frequencies are shown in Fig. 27b - 27d. The measured radiation pattern and realized gain agree well the simulation. Due to the loss of feeding lines with length differences up to tens wavelengths, there are variations of the realized gain for the TX antennas. However, one can always compensate such variations

of the TXs operating under the same mode by signal processing and calibration process. This is considered to be not critical for the overall performance of the IMR system.

Compared to [9] in which the same MIMO configuration was implemented by conventional waveguides, the gapwaveguide antenna system based on LiP technology has significant improvements in terms of:

1) Reduction of the ripples on azimuth pattern.
2) Assembly of multi-layer waveguides.
3) Integration with active circuits.

VII. CONCLUSION

An automotive IMR antenna using gapwaveguide technology is presented in this paper. A highly integrated radar transceiver utilizing LiP technology equipped with 4 RXs and 3 TXs is introduced. The transceiver is able to provide RF ports with waveguide interfaces, enabling direct integration with waveguide antennas. Robust interconnects for connecting transceivers to waveguide antennas with non-galvanic contact are proposed using gapwaveguide packaging technology. Compact transitions between RW and RGW are proposed to fan-out the feeding line. Designated antenna elements of the

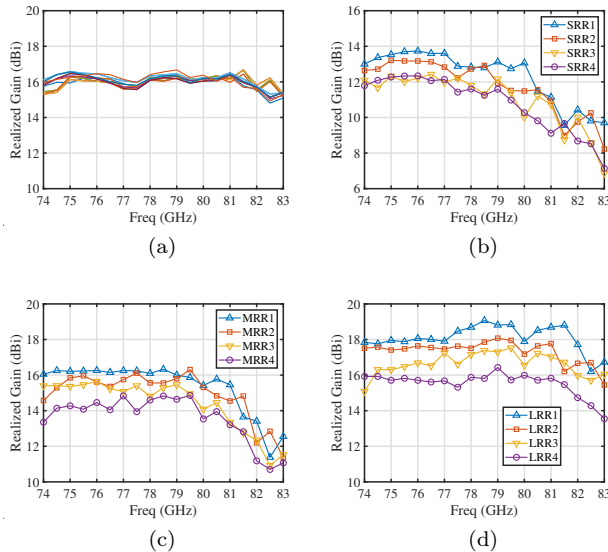**FIGURE 27.** Measured realized gain over frequency: (a) RXs with all 16 elements plotted together, (b) SRR, (c) MRR, (d) LRR.

system are realized by slot arrays with center-fed ridge gapwaveguides. Ultimately, the imaging radar antenna has a top radiating slot layer, a middle distribution layer and a bottom interconnect layer capable of accommodating 4 LiP components with considerable assembly tolerance. The interconnects are verified with launchers terminated by short or open loads. Good agreement between the simulation and measurement confirms the expected transmission properties of the interconnects. Input matching and radiation pattern of the antenna are also verified by measurement. The results indicate that the proposed antenna is able to serve the radar system properly.

REFERENCES

[1] J. Steinbaeck, C. Steger, G. Holweg, and N. Druml, "Next generation radar sensors in automotive sensor fusion systems," in 2017 Sensor Data Fusion: Trends, Solutions, Applications (SDF), 2017, pp. 1–6.

[2] F. de Ponte Müller, "Survey on ranging sensors and cooperative techniques for relative positioning of vehicles," Sensors, vol. 17, no. 2, p. 271, 2017.

[3] Texas Instruments, "MMWCAS-RF-EVM mmWave cascade imaging radar RF evaluation module," Accessed June 18, 2022. [Online]. Available: https://www.ti.com/tool/MMWCAS-RF-EVM

[4] A. Och, C. Pfeffer, J. Schrattenecker, S. Schuster, and R. Weigel, "A scalable 77 GHz massive MIMO FMCW radar by cascading fully-integrated transceivers," in 2018 Asia-Pacific Microwave Conference (APMC), 2018, pp. 1235–1237.

[5] B. J. Donnet and I. D. Longstaff, "MIMO radar, techniques and opportunities," in 2006 European Radar Conference, 2006, pp. 112–115.

[6] Continental Automotive, "Short Range Radar – SRR520," Accessed June 18, 2022. [Online]. Available: https://www.continental-automotive.com/en-gl/Passenger-Cars/Autonomous-Mobility/Enablers/Radars/Short-Range-Radar/SRR520

[7] AutonomouStuff, "Aptiv MRR," Accessed June 18, 2022. [Online]. Available: https://autonomoustuff.com/products/aptiv-mrr

[8] I. Bilik, S. Villeval, D. Brodeski, H. Ringel, O. Longman, P. Goswami, C. Y. B. Kumar, S. Rao, P. Swami, A. Jain, A. Kumar, S. Ram, K. Chitnis, Y. Dutt, A. Dubey, and S. Liu, "Automotive multi-mode cascaded radar data processing embedded system," in 2018 IEEE Radar Conference (RadarConf18), 2018, pp. 0372–0376.

[9] F. Jansen, F. Laghezza, S. Alhasson, P. Lok, L. van Meurs, R. Geraets, Ö. Paker, and J. Overdevest, "Simultaneous multi-mode automotive imaging radar using cascaded transceivers," in 2021 18th European Radar Conference (EuRAD), 2022, pp. 441–444.

[10] A. Vosoogh, A. Haddadi, A. U. Zaman, J. Yang, H. Zirath, and A. A. Kishk, "W -band low-profile monopulse slot array antenna based on gap waveguide corporate-feed network," IEEE Transactions on Antennas and Propagation, vol. 66, no. 12, pp. 6997–7009, 2018.

[11] A. Farahbakhsh, D. Zarifi, and A. U. Zaman, "60-GHz groove gap waveguide based wideband H -plane power dividers and transitions: For use in high-gain slot array antenna," IEEE Transactions on Microwave Theory and Techniques, vol. 65, no. 11, pp. 4111–4121, 2017.

[12] A. Haddadi, C. Bencivenni, and T. Emanuelsson, "Gap waveguide slot array antenna for automotive applications at E-band," in 2019 13th European Conference on Antennas and Propagation (EuCAP), 2019, pp. 1–4.

[13] M. Shih, C.-Y. Huang, T.-H. Chen, C.-C. Wang, D. Tarng, and C. P. Hung, "Electrical, thermal, and mechanical characterization of eWLB, fully molded fan-out package, and fan-out chip last package," IEEE Transactions on Components, Packaging and Manufacturing Technology, vol. 9, no. 9, pp. 1765–1775, 2019.

[14] W. Zhang, N. Li, J. Yu, and E. Kasper, "A compact single-board solution for commercializing cost-effective 77 GHz automotive front radar," in 2020 IEEE Asia-Pacific Microwave Conference (APMC), 2020, pp. 1098–1100.

[15] G. F. Hamberger, S. Späth, U. Siart, and T. F. Eibert, "A mixed circular/linear dual-polarized phased array concept for automotive radar—planar antenna designs and system evaluation at 78 GHz," IEEE Transactions on Antennas and Propagation, vol. 67, no. 3, pp. 1562–1572, 2019.

[16] S. Trummer, G. F. Hamberger, U. Siart, and T. F. Eibert, "A polarimetric 76–79 GHz radar-frontend for target classification in automotive use," in 2016 46th European Microwave Conference (EuMC), 2016, pp. 1493–1496.

[17] G. Carluccio, M. B. Vincent, M. Spella, A. J. M. de Graauw, and H. Thippur Shivamurthy, "Package," U.S. Patent 0 231 408A1, July 21, 2022. [Online]. Available: https://www.patentguru.com/search?q=US20220231408A1

[18] J. S. Häseker and M. Schneider, "90 degree microstrip to rectangular dielectric waveguide transition in the W-band," IEEE Microwave and Wireless Components Letters, vol. 26, no. 6, pp. 416–418, 2016.

[19] E. Topak, J. Hasch, and T. Zwick, "Compact topside millimeter-wave waveguide-to-microstrip transitions," IEEE Microwave and Wireless Components Letters, vol. 23, no. 12, pp. 641–643, 2013.

[20] Z. Tong and A. Stelzer, "A vertical transition between rectangular waveguide and coupled microstrip lines," IEEE Microwave and Wireless Components Letters, vol. 22, no. 5, pp. 251–253, 2012.

[21] E. Seler, M. Wojnowski, W. Hartner, W. Sörgel, J. Böck, R. Lachner, J. Hasch, and R. Weigel, "Chip-to-rectangular waveguide transition realized in embedded wafer level ball grid array (eWLB) package," in WAMICON 2014, 2014, pp. 1–4.

[22] A. U. Zaman, M. Alexanderson, T. Vukusic, and P.-S. Kildal, "Gap waveguide PMC packaging for improved isolation of circuit components in high-frequency microwave modules," IEEE Transactions on Components, Packaging and Manufacturing Technology, vol. 4, no. 1, pp. 16–25, 2014.

[23] A. Hassona, Z. S. He, V. Vassilev, C. Mariotti, S. E. Gunnarsson, F. Dielacher, and H. Zirath, "Demonstration of +100-

GHz interconnects in eWLB packaging technology," IEEE Transactions on Components, Packaging and Manufacturing Technology, vol. 9, no. 7, pp. 1406–1414, 2019.

[24] A. Hassona, Z. S. He, C. Mariotti, F. Dielacher, V. Vassilev, Y. Li, J. Oberhammer, and H. Zirath, "A non-galvanic D-band MMIC-to-waveguide transition using eWLB packaging technology," in 2017 IEEE MTT-S International Microwave Symposium (IMS), 2017, pp. 510–512.

[25] E. Seler, M. Wojnowski, W. Hartner, J. Böck, R. Lachner, R. Weigel, and A. Hagelauer, "3D rectangular waveguide integrated in embedded Wafer Level Ball Grid Array (eWLB) package," in 2014 IEEE 64th Electronic Components and Technology Conference (ECTC), 2014, pp. 956–962.

[26] U. Huegel, A. Garcia-Tejero, R. Glogowski, E. Willmann, M. Pieper, and F. Merli, "3D waveguide metallized plastic antennas aim to revolutionize automotive radar." Microwave Journal, vol. 65, no. 9, 2022.

[27] A. Mazzinghi, A. Freni, A. Agostini, L. Bossio, and M. Albani, "Industrial antenna development for 77-GHz level-crossing monitoring radar [antenna applications corner]," IEEE Antennas and Propagation Magazine, vol. 60, no. 5, pp. 95–106, 2018.

[28] NXP Semiconductors, "Fully Integrated 77 GHz RFCMOS Automotive Radar Transceiver," Accessed June 18, 2022. [Online]. Available: https://www.nxp.com/products/radio-frequency/radar-transceivers/fully-integrated-77-ghz-rfcmos-automotive-radar-transceiver:TEF82xx

[29] T. Braun, S. Raatz, U. Maass, M. Van Dijk, H. Walter, O. Hölck, K.-F. Becker, M. Töpper, R. Aschenbrenner, M. Wöhrmann, S. Voges, M. Huhn, K.-D. Lang, M. Wietstruck, R. F. Scholz, A. Mai, and M. Kaynak, "Development of a multi-project fan-out wafer level packaging platform," in 2017 IEEE 67th Electronic Components and Technology Conference (ECTC), 2017, pp. 1–7.

[30] K. Rambach and B. Yang, "MIMO radar: Time division multiplexing vs. code division multiplexing," in International Conference on Radar Systems (Radar 2017), 2017, pp. 1–5.

[31] F. Jansen, "Automotive radar doppler division MIMO with velocity ambiguity resolving capabilities," in 2019 16th European Radar Conference (EuRAD), 2019, pp. 245–248.

[32] N. Touati, C. Sturm, M. Imran, A. Vanaev, M. Kohler, K. Krupinski, W. Malik, and U. Lübbert, "High angle resolution automotive radar based on simultaneous 12Tx doppler-multiplex MIMO," in 2020 17th European Radar Conference (EuRAD), 2021, pp. 386–389.

QIANNAN REN received B.Sc. degree in electromagnetic field and wireless technology from University of Electronic Science and Technology of China, Chengdu, China, in 2016 and M. Sc. degree in electromagnetic field and microwave technology from Southeast University, Nanjing, China, in 2019. He is currently pursuing the Ph.D. degree at Chalmers University of Technology, Gothenburg, Sweden. His current research interests include millimeter wave antennas using gap waveguide technology, integration and packaging techniques for radar front-end and polarimetric radar systems.

CARLO BENCIVENNI is head of electrical engineer at Gapwaves. He has completed his PhD at Chalmers University of Technology in 2017 and since been working on mmwave antennas for communication and radar applications.

GIORGIO CARLUCCIO was born in 1979 and grew up in Ortelle, Italy. He received the Laurea degree in telecommunications engineering and the Ph.D. degree in information engineering from the University of Siena, Siena, Italy, in 2006 and 2010, respectively. In 2008 and 2009 he was an Invited Visiting Scholar with the ElectroScience Laboratory, Department of Electrical and Computer Engineering, The Ohio State University, Columbus, Ohio, USA. From 2010 to 2012 and from 2013 to 2014, he was a researcher with the Department of Information Engineering and Mathematics, University of Siena. From 2012 to 2013, he was a researcher with the Department of Electronics and Telecommunication, University of Florence, Florence, Italy. In 2012 and 2013 he was a visiting researcher with the Department of Microelectronics, Delft University of Technology (TU Delft), Delft, The Netherlands, where he also was a researcher from 2014 to 2018. Since 2018 he has been a RF circuits and antenna scientist with NXP Semiconductors, Eindhoven, The Netherlands, where he focuses on RF devices for automotive radar applications. His research interests deal with electromagnetic wave theory, mainly focused on asymptotic high-frequency techniques for electromagnetic scattering and propagation; and with modeling and design of antennas, quasi-optical systems, and periodic structures: mainly, reflector antennas, dielectric lens antennas, reflectarrays, connected arrays, THz antennas based on photoconductive materials, and antennas-in-package.

Dr. Carluccio was the recipient of the 2018 EurAAP International "Leopold B. Felsen Award for Excellence in Electrodynamics", and of the 2010 URSI Commission B Young Scientist Award at the International Symposium on Electromagnetic Theory (EMTS 2010), where he also received the third prize for the Young Scientist Best Paper Award.

HARSHITHA THIPPUR SHIVAMURTHY received the M.Sc. degree in electrical engineering from the Delft University of Technology (TU Delft), Delft, The Netherlands, in 2014, where she is currently pursuing the Ph.D. degree with the Terahertz Sensing Group. Her current research interests include analytical/numerical techniques in electromagnetics, design of integrated sensors for dielectric spectroscopy, and design of antenna arrays.

ANTON DE GRAAUW was born in Delft, The Netherlands, in 1966. He received the M.Sc. degree in electrical engineering from the Technical University of Delft, Delft, in 1993. He worked in several research and development positions at N.K.F. Telecom, Philips Components, Philips Semiconductors, and NXP Semiconductors, Eindhoven, The Netherlands, in the areas of fiber-optic CATV systems, RF and mm-Wave communication, and radar transceiver chips and antenna modules. He is currently an IC Architect in car-radar transceivers and integrated antennas at NXP Semiconductors.

FEIKE JANSEN was born in Eindhoven, The Netherlands, in 1980. He received the M.Sc. degree in electrical engineering from the Technical University of Eindhoven, Eindhoven, in 2006. In 2006, he joined Philips N.V., as a Researcher in the field of 24 GHz radar antennas. In 2007, he joined NXP Semiconductors N.V., where he is currently working as the Principal Scientist with the Algorithms and Software Innovation Group. There he worked on algorithm development for 60 GHz wireless communication basebands. Since several years, he has been working on algorithms and system design for 79 GHz automotive radar systems.
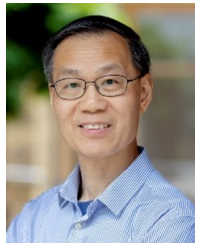
JIAN YANG (M'02-SM'10) received B.S. degree from the Nanjing University of Science and Technology, Nanjing, China, in 1982, and the M.S. degree from the Nanjing Research Center of Electronic Engineering, Nanjing, China, in 1985, both in electrical engineering, and the Swedish Licentiate and Ph.D. degrees from the Chalmers University of Technology, Gothenburg, Sweden, in 1998 and 2001, respectively. From 1985 to 1996, he was with the Nanjing Research Institute of Electronics Technology, Nanjing, China, as a Senior Engineer. From 1999 to 2005, he was with the Department of Electromagnetics, Chalmers University of Technology as a Research Engineer. During 2005 and 2006, he was with COMHAT AB as a Senior Engineer. From 2006 to 2010, he was an Assistant Professor at the Department of Signals and Systems, Chalmers University of Technology. From 2010, 2016 and 2020, he has been an associate professor, a professor, and a full professor, respectively, at the Department of Electrical Engineering, Chalmers University of Technology. He has published more than 80 journal articles and about 200 peer reviewed conference papers. H-index: 34 and i10-index: 90. His research interests include ultra-wideband antennas and UWB feeds for reflector antennas, mmWave antennas, mmWave multilayer phased array antennas, mmWave SWE (sheet waveguide element) antennas, Gap waveguide antennas, UWB radar systems, UWB antennas in near-field sensing applications, hat-fed antennas, reflector antennas, radome design, and computational electromagnetics.

ASHRAF UZ ZAMAN (SM'22) was born in Chittagong, Bangladesh. He received the M.Sc. and Ph.D. degrees from the Chalmers University of Technology, Gothenburg, Sweden, in 2007 and 2013, respectively. He is currently an Associate Professor with the Communication and Antenna Systems Division, Chalmers University of Technology. His current research interests include high gain millimeter-wave planar antennas, gap waveguide technology, frequency-selective surfaces, microwave passive components, RF packaging techniques and low-loss integration of MMICs with the active antennas. He is a member of the IEEE Microwave Theory and Techniques Society (MTT-S), the IEEE Antennas and Propagation Society (AP-S), and a reviewer of various IEEE and IET conferences and journals. He is also co-founder of the Chalmers startup company named Gapwaves AB and holds several patents.

∙ ∙ ∙